

UC Irvine

UC Irvine Previously Published Works

Title

Real-time Co-registered IVUS-OCT Catheter for Atherosclerotic Plaque Identification

Permalink

<https://escholarship.org/uc/item/9b69z033>

ISBN

9781467356862

Authors

Ma, Teng

Li, Jiawen

Jing, Joseph

et al.

Publication Date

2013-07-01

DOI

10.1109/ultsym.2013.0200

Copyright Information

This work is made available under the terms of a Creative Commons Attribution License, available at <https://creativecommons.org/licenses/by/4.0/>

Peer reviewed

Real-time Co-registered IVUS-OCT Catheter for Atherosclerotic Plaque Identification

Teng Ma¹, Jiawen Li², Joseph Jing², Xiang Li¹, Pranav M. Patel³, K. Kirk Shung¹, Zhongping Chen² and Qifa Zhou¹

1. NIH Ultrasonic Transducer Resource Center and Department of Biomedical Engineering,
University of Southern California, Los Angeles, California, USA

2. Beckman Laser Institute & Medical Clinic and Department of Biomedical Engineering,
University of California – Irvine, Irvine, California, USA

3. Division of Cardiology, UC Irvine Medical Center, Irvine, California, USA

Abstract—Coronary artery disease remains the leading cause of death and disability in the US. Intravascular ultrasound (IVUS) is one of the standard medical tests routinely performed in hospital to diagnose atherosclerosis by visualizing the structure of affected vessels and identifying the composition of plaques. Optical coherence tomography (OCT) possesses higher resolution to image vulnerable plaque near the lumen boundary, but with a shallow penetration depth. Thus, an integrated IVUS-OCT catheter would potentially capitalize the advantage of sufficient imaging depth of IVUS and the high resolution of OCT while offering improved diagnostic information. Different IVUS-OCT catheter designs have been reported previously by using either co-axial, co-planner or sequential configuration, which suffers from either the large size of catheter or suboptimal image co-registration. By placing the OCT probe and 45MHz single element IVUS transducer back-to-back at the same axial direction, this probe can provide automatically co-registered, co-axial IVUS-OCT imaging. To demonstrate its capability, IVUS-OCT imaging of major types of advanced plaques in human cadaver coronary segments was obtained using this catheter and system. Results were validated by histology analysis.

Keywords—ultrasonic transducer, intravascular ultrasound, optical coherence tomography, catheter

I. INTRODUCTION

Atherosclerosis, a condition in which an artery wall thickens as a result of the accumulation of fatty materials such as cholesterol, is the leading cause of morbidity and mortality in developed countries [1]. Acute coronary syndrome (ACS) is caused by the progression of vulnerable atherosclerotic plaques within coronary artery walls. Thin-cap fibroatheroma (TCFA), as a specific and major cause of ACS, has the morphologic features of a thin fibrous cap less than 65 microns followed by numerous macrophages within the cap and a large necrotic core [2]. Thus, it is essential to have high resolution and deep penetration imaging technique to resolve the vulnerable plaque elements. Intravascular ultrasound (IVUS) is one of the standard medical tests routinely performed to diagnose atherosclerosis by visualizing the whole structure of affected vessels and identifying the composition of

plaques. Optical coherence tomography (OCT) possesses high resolution to image vulnerable plaque near the lumen boundary, but with shallow penetration depth [3]. However, due to intrinsic limitations of resolution and penetration depth, respectively, neither IVUS nor OCT alone is able to accurately assess of plaque characteristics [4]. Thus, an integrated IVUS-OCT catheter would potentially capitalize the advantage of sufficient imaging depth of IVUS with the high resolution of OCT while offering improved diagnostic information.

The combined use of separately obtained IVUS-OCT images has been demonstrated to improve the capability for TCFA recognition [4]. The major limitation is the offline fusion procedures of IVUS and OCT images, which not only expands the operation and diagnosis time but also causes errors due to inaccurate co-registration. Thus, to overcome the limitation, a fully-integrated IVUS-OCT imaging system is indeed necessary to achieve *in vivo* assessment of vulnerable plaques.

In prior studies, different IVUS-OCT catheter designs have been reported by using co-axial, co-planner or sequential configuration, which suffers from either the large size of catheter or suboptimal image co-registration. Li et al [5] reported a probe with confocal configuration of ultrasound beam and laser light to accomplish the first online co-registered imaging capability; however, with the outer diameter of over 2.4 mm, the probe is too large to be used in intracoronary artery imaging. The first successful *in vivo* animal studies were reported by Yin et al [6] to demonstrate the feasibility of integrated IVUS-OCT by using a miniature probe fitted in a 3.6-Fr catheter sheath. However, one limitation of this probe is that the optic fiber and electrical wire were sealed in a rigid steel tube of more than 5 mm long, which significantly downgraded the probe's flexibility. Moreover, since there were 2 mm offset between the OCT prism and IVUS transducer, the imaging co-registration had to rely on offline processing to shift the two images to the same region of interest (ROI). Given the shape of lumens constantly within cardiac cycle, the IVUS and OCT images acquired at different time points could not always be accurately co-registered during the *in vivo* study.

In this paper, we present a novel design of a miniature integrated catheter using back-to-back arrangement of OCT and IVUS probes to facilitate imaging at the same ROI simultaneously. This catheter enables real-time imaging and

display of co-registered IVUS-OCT images for identifying vulnerable plaques and guiding coronary intervention, which better fits clinical needs compared to the previous probe designs with an offline fusion method. In addition, this probe design has the same rigid-part size as the clinically-used IVUS or OCT probe, with a clinically acceptable outer diameter (OD), without sacrificing image quality. The reduction in probe size is essential to enable safer IVUS-OCT imaging in clinical settings. Images of major types of advanced atherosclerotic plaques in human cadaver coronary segments further demonstrate the imaging capability of this novel probe.

II. EXPERIMENTAL ARRANGEMENT

A. Integrated IVUS-OCT Imaging System

Fig.1 shows the schematic of the integrated imaging system. The imaging system is composed of four parts: OCT sub-system, IVUS sub-system, data acquisition and processing, and integrated catheter with rotary unit.

For the OCT sub-system, light from the 1310 nm swept source was split by a coupler with 80% of power directed into the catheter. The measured sensitivity of OCT was 103 dB. For the IVUS sub-system, a Panametrics PR5900 pulser/receiver (Olympus NDT, Kennewick, WA) was used for pulse generation and signal detection with 26 dB gain and 10~100 MHz band-pass filter. The laser source was used to generate 20 kHz trigger signals which drove a function generator to synchronize the digitizer and the pulser/receiver. IVUS and OCT signals were fed into separate channels of the 12 bit digitizer and digitized at a sampling rate of 200 MHz. The sampling clock was provided by an external voltage controlled oscillator (VCO). The acquired IVUS and OCT signals were processed, displayed and saved in real time by custom built software. The system has a frame rate of 10 frs/s with 1000 A-lines per frame. A custom built rotary joint device was used for motion control and signal coupling from the rotational part to the stationary part. A fiber optic rotary joint (Princetel, Inc., Pennington, New Jersey) and an electrical slip ring (Prosperous, Co., Hangzhou, China) were used for signal coupling. All these components were fixed to a translational stepper motor with pull-back capability.

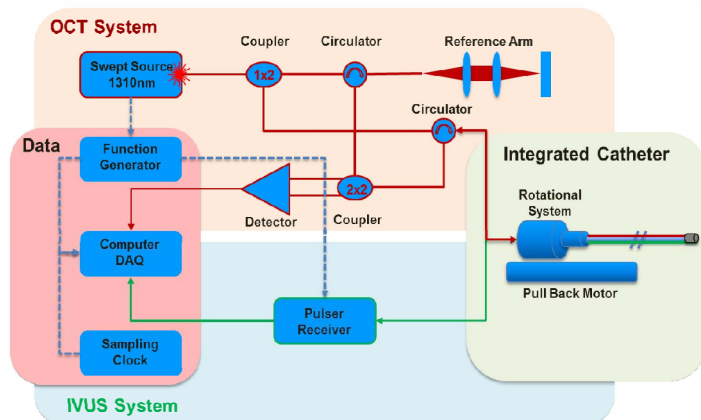


Fig.1. Schematic of the integrated imaging system.

B. Back-to-back Catheter Design

The schematic of back-to-back IVUS-OCT catheter is shown in Fig.2 (a). Within the OCT probe, a 0.35 mm-diameter gradient index (GRIN) lens (NSG America, Inc., Somerset, NJ) was used for light focusing, followed by a 0.3 mm-diameter micro-prism (Tower Optical Corp., Boynton Beach, FL). The working distance of the OCT probe was about 3 mm.

The IVUS transducer was fabricated based on the $\text{PbMg}_{1/3}\text{Nb}_{2/3}\text{O}_3\text{-PbTiO}_3$ (PMN-PT) single crystal with high piezoelectric coefficient (2000 pC/N) and electromechanical coupling coefficient (0.58) [7]. The PMN-PT plate was lapped to the designed thickness of 40 μm for 45 MHz with 1500 \AA chrome/gold (Cr/Au) layers as electrodes coated on both sides. A 10 μm matching layer made of a mixture of Insulate 501 epoxy (American Safety Technologies, Roseland, NJ) and 2-3 μm silver particle (Sigma-Aldrich Inc., St. Louis, MO, USA) was casted onto the front side of PMN-PT plate. The conductive backing made of silver epoxy (E-Solder 3022, Von Roll Isola Inc, New Haven, CT) was cast and centrifuged onto the back side of PMN-PT plate. The matched/backed plate was finally lapped to a thickness of only 300 μm before mechanically dicing into 0.4 mm \times 0.4 mm square shape. A center core of a 46 AWG coaxial cable was connected to the side of the backing layer (back electrode) and covered by epoxy (Epo-Tek 301, Epoxy Technologies, Billerica, MA) to insulate from the front electrode without increasing the thickness of transducer. The front surface of the matching layer was connected to the metallic shield of coaxial cable with Cr/Au for grounding connection. A parylene layer of 12 μm thick was vapor-deposited on to the transducer to serve as the second matching and waterproof layer.

With the guidance of visible light from the OCT-sub probe, the transducer was carefully aligned on OCT sub-probe, while confirming that the light beam and sound wave exit at the same axial position, but 180 degrees apart. The gap between the transducer and housing was filled with epoxy to reinforce stability. Finally, the proximal end of the coaxial cable was connected to a slip ring to enable rotational scan capability. This integrated probe provides automatically co-registered and co-axial fusion imaging. The combined probe was then inserted into customized probe housing (a stainless steel tube with two windows; OD: 0.9 mm; length: 2 mm). The flexible torque coil ensures accurate and smooth translation of torque to the distal end over a large distance and through tortuous curves. During experiments, the probe was inserted into a sheath to avoid cross-contamination between probe and cadaver segments. Distilled water was filled in the sheath before experiments.

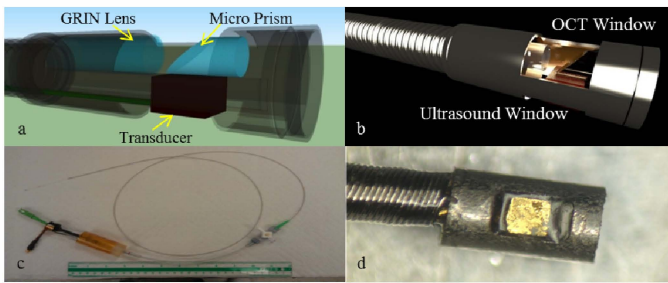


Fig.2. (a) Schematic of the back-to-back IVUS-OCT probes (b) 3D rendering image of catheter tip with a housing (OD: 0.9mm, length 2mm) (c) photo of the whole catheter (d) photo of the back-to-back probe, showing the transducer side.

C. *In vitro* imaging of human atherosclerosis

To test the catheter's capability, *in vitro* imaging on human coronary artery samples were conducted. All Imaging was performed at 1000 pixels per frame, 10 frames per second. The co-registered OCT-IVUS image pairs were displayed in real-time, by rotating OCT images 180 degrees to match IVUS images' orientation. Plaques located at middle to proximal part of arteries were imaged with this OCT-IVUS integrated system in saline. After imaging, each coronary artery segment was sectioned for Hematoxylin-Eosin (H&E) histology analysis.

III. RESULTS AND DISCUSSIONS

A. Transducer performance

The pulse-echo response and frequency spectra of the PMN-PT transducer are shown in Fig. 3. It was found that the measured center frequency of the transducer is around 45 MHz. The f_1 and f_2 of the transducer were found to be 37 MHz and 54 MHz, respectively. The -6 dB fractional bandwidth was determined to be ~ 40 %. Fig. 4 shows the modeled result of the PMN-PT transducer which was performed using PIEZOCAD. The modeled results show that the modeled center frequency and -6 dB bandwidth are 45 MHz and ~ 41 %, respectively. The comparison shows that the measured data are in reasonably good agreement with the modeled results to provide satisfactory IVUS images.

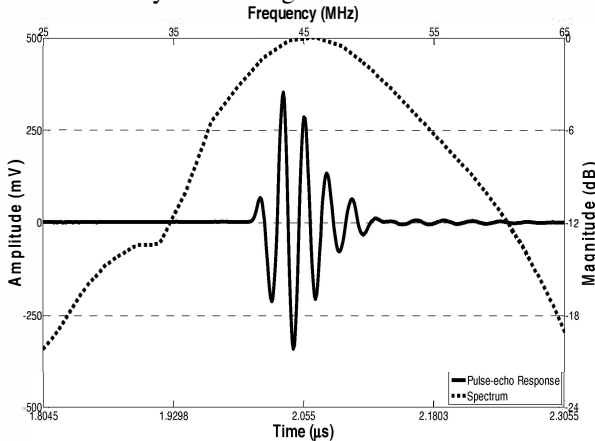


Fig. 3. Time-domain pulse / echo response and frequency spectrum of the 45 MHz IVUS transducer.

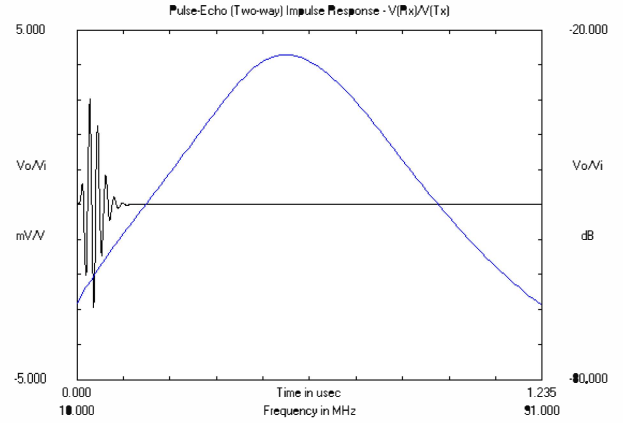


Fig. 4. Modeled pulse / echo response of the 45 MHz IVUS transducer.

B. *In vitro* imaging of human atherosclerosis

In vitro IVUS and OCT images acquired from the integrated IVUS-OCT catheter on a segment of human cadaver sample is shown in Fig.5. The H&E histology image [Fig.5 (d)] shows that there are several small calcified plaques (black arrow) and eccentric intimal thickening (green arrow). In the IVUS image [Fig.5 (a)], the bright border followed by a large acoustic shadow confirms the existing of calcified plaques. However, due to the insufficient resolution and acoustic scattering contrast, the shapes of the two small calcified plaques are hardly differentiated. The OCT image [Fig. 5 (b)] can clearly identify the superficial calcification with a sharp boundary, and the two small calcified plaques can be clearly separated. The resolved structures of the two plaques agree with the histology results. Even though OCT image can clearly visualize the lumen boundary and the intimal thickening region, the whole vascular structure is not well identified due to the shallow penetration depth of OCT. The corresponding IVUS image not only shows the shape and size of the intimal thickening region, but also provides a visualization of media and adventitia layers. The fused image in Fig.5 (c) shows that IVUS and OCT images match well, which demonstrates the catheter's online co-registration capability. The high resolution information near the lumen boundary and the deep penetration through the whole vessel wall provide an improved assessment of the plaque structure compared with either modality alone.

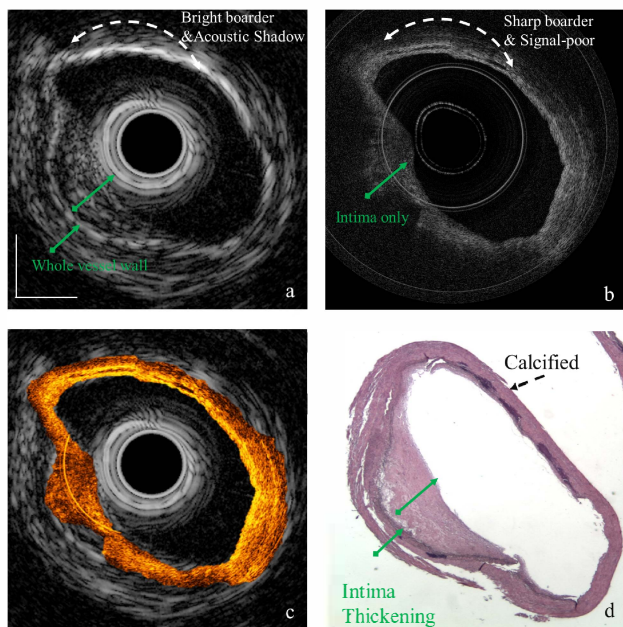


Fig. 5. (a) OCT image, (b) IVUS image, (c) fused IVUS-OCT image, and (d) corresponding H&E histology image of an atherosclerotic human coronary artery with eccentric plaque. The white arrow indicates the small calcified plaque and the green arrow points to an intimal thickening region.

IV. CONCLUSIONS

In summary, a novel miniaturized probe for automatically co-registered IVUS-OCT imaging has been developed. With our present probe and system, IVUS-OCT imaging with online real-time fusion has been achieved, which demonstrates the co-registered nature of this probe and the real-time polar image display capability of this system. Human plaques' morphologic characteristics were also clearly imaged. This design enables real-time *in situ* characterization of plaques and guiding of coronary intervention, which is essential in translating this technology from bench to clinical applications.

V. ACKNOWLEDGEMENTS

The project described was supported by NIH (UL1 RR031985, R01EB10090, R01EB-00293, R01HL105215, RR-

01192, and P41-EB2182) and the U.S. Air Force Office of Scientific Research, Medical Free-Electron Laser Program FA9550-08-1-0384. Institutional support from the Beckman Laser Institute Endowment is also gratefully acknowledged.

VI. REFERENCES

- [1] R. Puri, M. I. Worthley, and S. J. Nicholls, "Intravascular imaging of vulnerable coronary plaque: current and future concepts," *Nat. Rev. Cardiol.*, vol. 8, no. 3, pp. 131-139, 2011.
- [2] R. Virmani, F. D. Kolodgie, A. P. Burke, A. Farb, and S. M. Schwartz, "Lessons from sudden coronary death: a comprehensive morphological classification scheme for atherosclerotic lesions," *Arterioscler. Thromb. Vasc. Bio.*, vol. 20, no. 5, pp. 1262-1275, 2000.
- [3] G. Pasterkamp, E. Falk, H. Woutman, and C. Borst, "Techniques characterizing the coronary atherosclerotic plaque: Influence on clinical decision making," *J. Am. Coll. Cardiol.* vol. 36, pp. 13-21, 2000.
- [4] T. Sawada, J. Shite, H. M. Garcia-Garcia, T. Shinke, S. Watanabe, H. Otake, D. Matsumoto, Y. Tanino, D. Ogasawara, H. Kawamori, H. Kato, N. Miyoshi, M. Yokoyama, P. W. Serruys, and K. Hirata, "Feasibility of combined use of intravascular ultrasound radiofrequency data analysis and optical coherence tomography for detecting thin-cap fibroatheroma," *Eur. Heart J.*, vol. 29, no. 9, pp. 1136-1146, 2008.
- [5] X. Li, J. Yin, C. Hu, Q. Zhou, K. K. Shung, and Z. Chen, "High-resolution coregistered intravascular imaging with integrated ultrasound and optical coherence tomography probe," *Appl. Phys. Lett.*, vol. 97, no. 13, pp. 133702, 2010.
- [6] J. Yin, X. Li, J. Jing, J. Li, D. Mukai, S. Mahon, A. Edris, K. Hoang, K. K. Shung, M. Brenner, J. Narula, Q. Zhou, and Z. Chen, "Novel combined miniature optical coherence tomography ultrasound probe for in vivo intravascular imaging," *J. Biomed. Opt.* vol. 16, no.6, 060505, 2011.
- [7] J. Tian, P. D. Han, and D. A. Payne, "Measurements along the growth direction of PMN-PT crystals: dielectric, piezoelectric, and elastic properties," *IEEE Trans. Ultra. Ferro. Freq. Ctr.*, vol. 54, no. 9, pp. 1895-1902, 2007.